

LIQUID METAL-BASED FLEXIBLE BAND-STOP FREQUENCY SELECTIVE SURFACE

Arkadeep Mitra¹, Kevin Xu², Sachin Babu¹, Jun H. Choi² and Jeong-Bong Lee^{1,*}

¹Department of Electrical and Computer Engineering,

University of Texas at Dallas, Richardson, Texas, USA

²Department of Electrical Engineering, University at Buffalo, Buffalo, New York, USA

ABSTRACT

We report the design, fabrication, and characterization of PDMS encapsulated physically flexible (bendable, foldable) gallium-based liquid metal band-stop frequency selective surface. A band-stop frequency selective surface (FSS) with targeted operation in the X-band (7~11.2 GHz) was designed. Liquid metal was embedded in PDMS microfluidic channels replicated from a deep etched Si mold. Ultra-low pressure (5.75×10^{-6} Torr) vacuum at cryogenic temperatures (10 K) was employed for clean encapsulation of liquid metal. An array of 5 x 5 FSS has been fabricated. Characterization of the fabricated FSS was carried out in a waveguide environment. The S-parameter values of the simulated and measured band-stop FSS response showed an excellent agreement.

KEYWORDS

PDMS, liquid metal, band-stop, flexible, frequency selective surface.

INTRODUCTION

Frequency selective surface (FSS) is a periodic array structure of sub wavelength metallic elements on dielectric surface in one or two-dimension [1-2]. FSSs are broadly classified into high pass, band-pass, band-stop and low pass filters [3-4] based on geometry [4], physical construction and material [5].

Alike a spatial filter, FSS allows the transmission, absorption, or reflection of electromagnetic waves. Characteristics of a FSS largely depends on the frequency band for which it is designed to operate. The response towards the respective frequency band results in the generation of scattered waves. FSS performance is influenced by the surrounding metallic frames, array number, periodicity, substrate conductivity, and geometry [5]. FSS forms an indispensable component of communication system involving radar, satellite communication and wireless networks.

Gallium-based liquid metal has been one of the emerging materials in recent years. A variety of applications has been demonstrated due to its metallic property combined with its liquid property along with its biocompatibility. One of the interesting applications is use of liquid metal as “deformable” metallic conductors for soft/flexible electronics applications [6].

Liquid metal has been used in FSS, but previous works were all based on FSS fabrication in rigid substrates [7]. In this paper, we report a liquid metal-based physically flexible (bendable, foldable) band-stop FSS in the X-band. To the best of our knowledge this is the first experimental demonstration of a mechanically

flexible liquid metal-based band-stop FSS.

DESIGN

The liquid metal-based band-stop FSS unit cell is designed to have a Jerusalem cross loaded with a floating parasitic patch next to each end cap, as shown in Figure 1. The 200 μm thick liquid metal layer made of Galinstan (conductivity $\sigma = 3.46 \times 10^6 \text{ S/m}$) is embedded in PDMS (relative permittivity $\epsilon_r = 2.3$ and loss tangent $\tan \delta = 0.02$) and filled through a layer of holes located directly above.

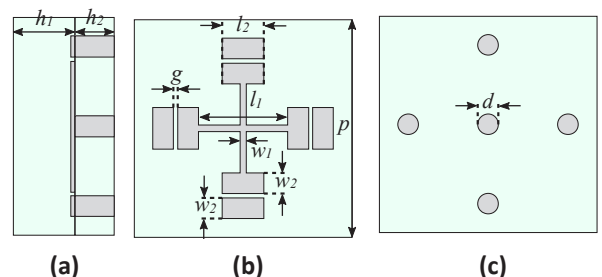


Figure 1: Liquid metal band-stop FSS unit cell in PDMS: (a) side view ($h_1=2.95 \text{ mm}$ and $h_2=1.9 \text{ mm}$), (b) modified Jerusalem cross layer ($l_1=4.3 \text{ mm}$, $w_1=0.3 \text{ mm}$, $l_2=2 \text{ mm}$, $w_2=1 \text{ mm}$, $g=0.2 \text{ mm}$ and $p=10.5 \text{ mm}$), (c) liquid metal filled hole array ($d=1 \text{ mm}$).

The liquid metal-based band-stop FSS design has been simulated using ANSYS HFSS. In the simulation, an infinite 2D array of FSS unit cell was used. The transmission and reflection coefficient at normal angle of incidence with peak band-stop characteristic slightly below 10 GHz are shown in Figure 2.

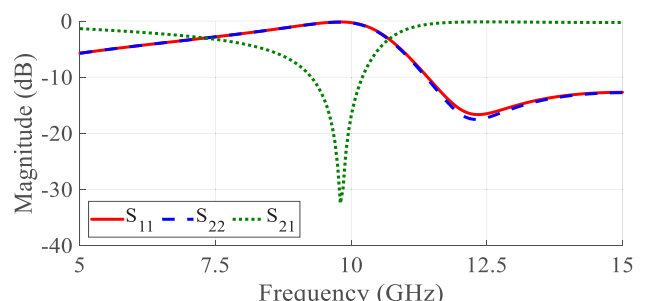


Figure 2: Simulated band-stop FSS results.

FABRICATION

Fabrication sequence of the designed FSS is shown in Figure 3. Fabrication has been started with Microposit® S1813 spin coating and patterning on a 4-inch bare silicon wafer. Following evaporation and photoresist liftoff, Chromium hard mask (Fig. 3a) was formed. Deep silicon

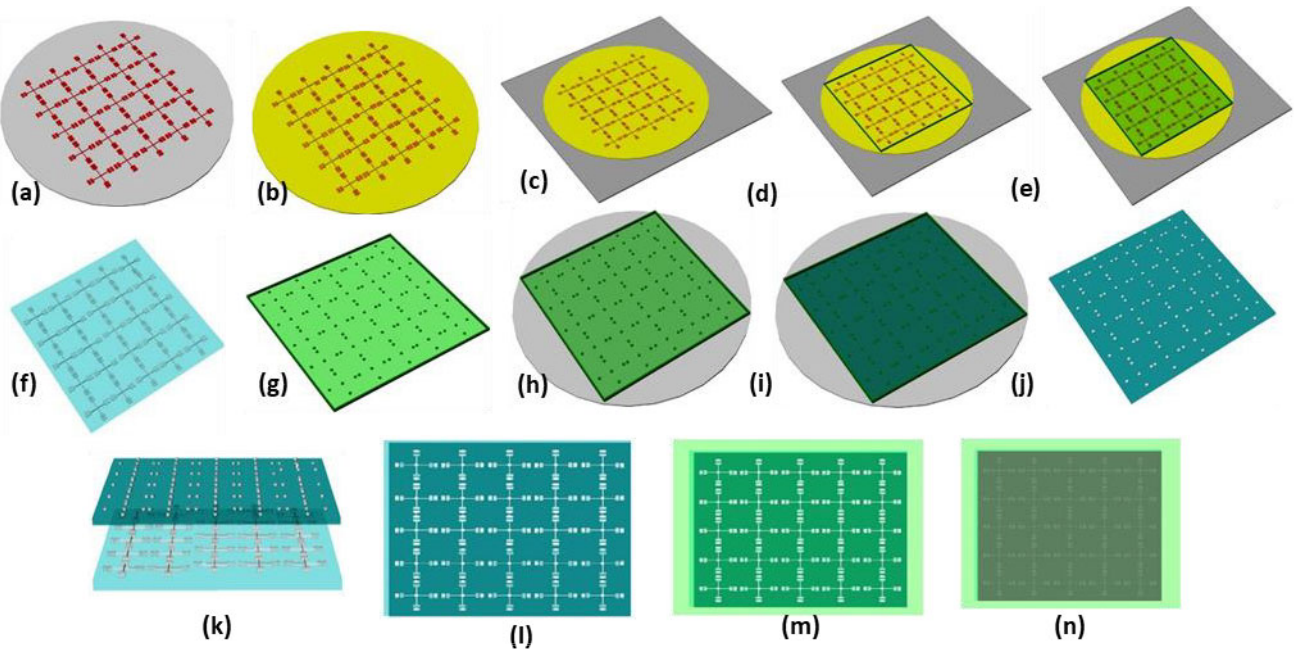


Figure 3: Fabrication sequence of FSS structures in ultra-low pressure: (a) Chromium hard mask on Si, (b) Teflon coated Si, (c) Si attached to scrap mask, (d) 3D borders attached to Si wafer, (e) PDMS poured on Si mold, (f) cured FSS-PDMS, (g) 3D pillar array mold, (h) pillar array mold attached to Si wafer, (i) PDMS poured on pillar array mold, (j) cured hole-array PDMS, (k) alignment of hole-array PDMS on FSS-PDMS, (l) bonded structure, (m) bonded structure placed in open top 3D container, (n) 3D container flooded with Galinstan.

plasma etching has been performed to form a 5 x 5 array FSS unit cells. PDMS was spin coated on a scrap mask and Teflon coated Si wafer was placed over it (Fig. 3b-c). A square shaped 3D printed border of 2 mm height was glued using Devcon epoxy (Fig. 3d) around the FSS array. FSS-PDMS was replicated from the Si mold (Fig. 3e-f). To have efficient injection of liquid metal into the FSS pattern, 3D printed pillar array of 1 mm diameter (Fig. 3g) with heights higher than the borders was attached to the Si wafer using Devcon epoxy (Fig. 3h). Hole-array PDMS was replicated from the 3D pillar array mold (Fig. 3i-j).

Following alignment, the hole-array PDMS and FSS-PDMS were plasma bonded and cured (Fig. 3k-l). The hole-array PDMS was flooded with Galinstan (GaInSn eutectic alloy, 99.99%), after placement on an open top 3D printed container (Fig. 3m-n). The container was loaded into a high vacuum chamber and subjected to pressure in range of 10^{-6} Torr vacuum at cryogenic temperatures (9~12 K) for 2 hours. Following venting, Galinstan filling took place in the PDMS microfluidic FSS structures through the hole array because of the positive pressure difference introduced by the atmospheric pressure. Following hole-array surface cleaning, PDMS was used to seal off the holes and cured at room temperature (Fig. 4a).

One of the common problems in liquid metal injection in microfluidic channel is air bubbles. The vacuum filling technique we used fills liquid metal into a large array of the delicate FSS microfluidic channels and does not allow air pockets when compared to conventional injection filling [8]. We found that a combination of ultra-high vacuum and filling in cryogenic temperature could completely fizz out air bubbles. Air bubbles are serious problems in structures like FSS as its RF (radio frequency) characteristics is significantly

compromised with irregular placements of air pockets in a structure that should be periodic.

In the final fabrication step, the PDMS hole array was peeled away that leaves behind FSS-PDMS layer (Fig. 4b). A thorough examination was done to study the effectiveness of the gallium oxide adhesion with respect to FSS-PDMS layer under no stretch/stretch condition. The adhesion was also examined with respect to the flexibility of the FSS-PDMS by placing the bare liquid metal filled FSS-PDMS array in a vertical position. Repeated bending experiments were performed. According to the observation, liquid metal did not seep out of the FSS-PDMS structures demonstrating the complete encapsulation of the liquid metal in PDMS.

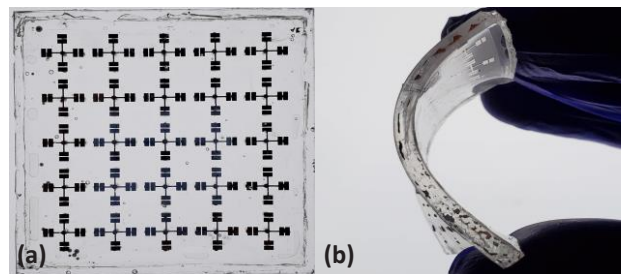


Figure 4: Liquid metal filled FSS structure by vacuum filling and post cleaning (a) top view, (b) side view demonstrating flexibility and lyophilicity.

CHARACTERIZATION

The fabricated liquid metal encapsulated PDMS FSS has been characterized using a waveguide measurement setup around 8 ~ 13 GHz. We used a sample size equal to the inner dimensions of the WR-90 waveguide (22.86 mm x 10.16 mm), which is approximately the size of a 1x2

array. The sample was cut and placed inside a waveguide shim milled out of 6.35 mm thick aluminum. The measurement setup, sample holder, and the fabricated liquid metal-based band-stop FSS sample are shown in Figure 5. Two ports of a Keysight N5242A PNA-X network analyzer have been connected through waveguide to coax adapters to measure S-parameters calibrated up to the sample.

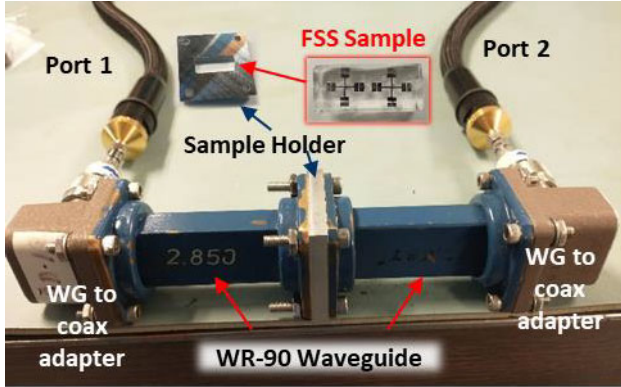


Figure 5: Waveguide measurement setup for the FSS sample using WR-90 waveguide.

To have precise measurement of the FSS, the hole array (Fig. 6a) on top of 1 x 2 FSS array was removed which leaves the 1 x 2 band-stop FSS array (Fig. 6b).

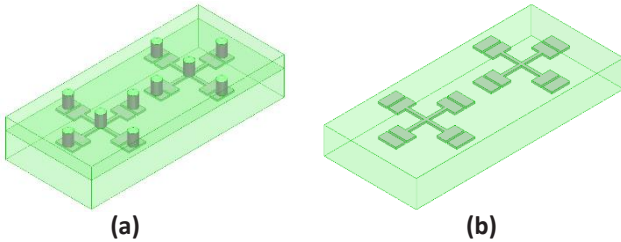


Figure 6: Liquid metal bandstop FSS sample structure (a) before and (b) after removing the hole array layer.

For sake of comparison, simulation of the 1 x 2 FSS array used for measurement inside the WR-90 waveguide was also performed. Comparison of measured and simulated results of the FSS with hole array removed, is shown in Figure 7. Excellent agreement between the simulated and measured results can be seen with clear band-stop characteristic peak at around 11 GHz, which was slightly (~10%) shifted from its originally designed operation frequency (Fig. 2).

CONCLUSION

In this work, feasibility of fabricating large scale (5 x 5 array) liquid metal encapsulated physically flexible FSS structure was demonstrated using ultra-high vacuum at cryogenic temperature has been demonstrated. The simulated and measured response of the band-stop FSS in the X-band showed excellent agreement. The hole-array PDMS was peeled off during characterization, opening the possibility of using this facile fabrication methodology further for integrating an even larger array FSS structure.

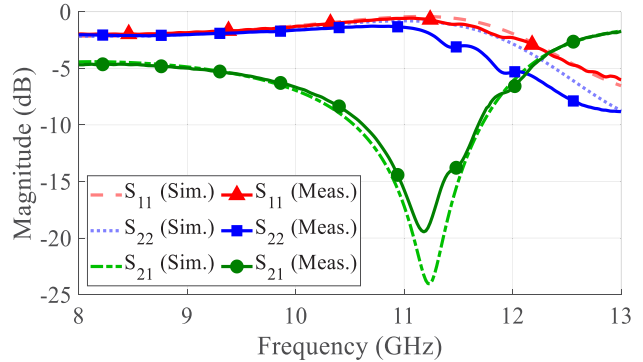


Figure 7: Simulated and measured response of FSS sample with hole array removed in WR-90 waveguide.

Although this paper focuses on the experimental verification of a FSS at a fixed frequency in the X-band, the floating patches are incorporated into the design as a potential tuning element for actively tuned FSSs. We envision a large array physically flexible (bendable, foldable) on-demand dynamically tunable FSS using liquid metal in microfluidic channel as a tuning element which can be used in a wide variety of communication and military applications.

ACKNOWLEDGEMENTS

This work was supported in part by the United States National Science Foundation grant NSF ECCS-1908779. The authors would also like to acknowledge UT Dallas Clean Room staff for their support on this work.

REFERENCES

- [1] K. Payne, K. Xu and J. H. Choi, "Generalized synthesized technique for the design of thickness customizable high-order bandpass frequency-selective surface", *IEEE Transactions on Microwave Theory and Techniques*, vol. 66, pp. 4783-4793, 2018.
- [2] N. Behdad, "A second-order band-pass frequency selective surface using nonresonant subwavelength periodic structures", *Microwave and Optical Technology Letters*, vol. 50, pp. 1639-1643, 2008.
- [3] H. Nemat-Abad, E. Zareian-Jahromi and R. Basiri, "Design and equivalent circuit model extraction of a third order band-pass frequency selective surface filter for terahertz applications", *Engineering Science and Technology, an International Journal*, vol. 22, pp. 862-868, 2019.
- [4] S. N. Azemi and W. S. Rowe, "Development and analysis of 3D frequency selective surfaces", in *Proc. Asia-Pacific Microwave Conference*, Melbourne, December 5-8, 2011, pp. 693-696.
- [5] R. S. Anwar, L. Mao, and H. Ning, "Frequency selective surfaces: a review", *Applied Sciences*, vol. 8, pp. 1689, 2018.
- [6] M. D. Dickey, R. C. Chiechi, R. L. E. A. Weiss, D. A. Weitz, and G. M. Whitesides, "Eutectic gallium-indium (EGaIn): a liquid metal alloy for the formation of stable structures in microchannels at

room temperature”, *Advanced functional materials*, vol. 18, pp. 1097-1104, 2008.

[7] M. Li and N. Behdad, “Fluidically tunable frequency selective/phase shifting surfaces for high-power microwave applications”, *IEEE Transactions on Antennas and Propagation*, vol. 60, pp. 2748-2759, 2012.

[8] Y. Lin, O. Gordon, M. R. Khan, N. Vasquez, J. Genzer, and M. D. Dickey, “Vacuum filling of complex microchannels with liquid metal”, *Lab on a Chip*, vol. 17, pp. 3043-3050, 2017.

CONTACT

*Jeong Bong (JB) Lee, tel: +1-972-883-2893;
jblee@utdallas.edu